Journal of Visualized Experiments

A Three-Dimensional Spheroid Model to Investigate the Tumor-Stromal Interaction in Hepatocellular Carcinoma

--Manuscript Draft--

Article Type:	Invited Methods Article - JoVE Produced Video
Manuscript Number:	JoVE62868R2
Full Title:	A Three-Dimensional Spheroid Model to Investigate the Tumor-Stromal Interaction in Hepatocellular Carcinoma
Corresponding Author:	Marco Zaki, PhD Minia University Faculty of Pharmacology Minia, Minia EGYPT
Corresponding Author's Institution:	Minia University Faculty of Pharmacology
Corresponding Author E-Mail:	marcozaki@mu.edu.eg
Order of Authors:	Marco Zaki, PhD
	Shishir Shetty
	Alex Wilkinson
	Daniel Patten
	Fiona Oakley
	Helen Reeves
Additional Information:	
Question	**Response**
Please specify the section of the submitted manuscript.	Cancer Research
Please indicate whether this article will be Standard Access or Open Access.	Open Access ($3900)
Please indicate the **city, state/province, and country** where this article will be **filmed**. Please do not use abbreviations.	Birmingham, United Kingdom
Please confirm that you have read and agree to the terms and conditions of the author license agreement that applies below:	I agree to the UK Author License Agreement (for UK authors only)
Please provide any comments to the journal here.	
Please confirm that you have read and agree to the terms and conditions of the video release that applies below:	I agree to the Video Release

TITLE:

A Three-Dimensional Spheroid Model to Investigate the Tumor-Stromal Interaction in Hepatocellular Carcinoma

AUTHORS AND AFFILIATIONS:

Marco Y. W. Zaki[1,2#]*, Shishir Shetty[2#], Alex L. Wilkinson[2], Daniel A. Patten[2], Fiona Oakley[3$], Helen Reeves[4,5$]

[1]Department of Biochemistry, Faculty of Pharmacy, Minia University, Minia, Egypt
[2]National Institute for Health Research Birmingham Liver Biomedical Research Unit and Centre for Liver and Gastrointestinal Research, Institute of Immunology and Immunotherapy, University of Birmingham, Birmingham, United Kingdom
[3]Newcastle Fibrosis Research Group, Biosciences Institute, Faculty of Medical Sciences, Newcastle University, Newcastle-upon-Tyne, UK
[4]Newcastle University Translational and Clinical Research Institute, Faculty of Medical Sciences, Newcastle University, Newcastle-upon-Tyne, UK
[5]The Liver Unit, Department of Medicine, Freeman Hospital, Newcastle-upon-Tyne Hospitals NHS Foundation Trust, Newcastle upon Tyne, UK

Email addresses of the authors:

Marco Y. W. Zaki	(marcozaki@mu.edu.eg)
Shishir Shetty	(S.Shetty@bham.ac.uk)
Alex L. Wilkinson	(axw717@student.bham.ac.uk)
Daniel A. Patten	(D.A.Patten@bham.ac.uk)
Fiona Oakley	(fiona.oakley@newcastle.ac.uk)
Helen Reeves	(helen.reeves@newcastle.ac.uk)

*Email address of the corresponding author:

Marco Y. W. Zaki	(marcozaki@mu.edu.eg)

[#]Authors sharing the first authorship

[$]Authors sharing the last authorship

SUMMARY:

Comprehensive *in vitro* models that faithfully recapitulate the relevant human disease are lacking. The current study presents three-dimensional (3D) tumor spheroid creation and culture, a reliable *in vitro* tool to study the tumor-stromal interaction in human hepatocellular carcinoma.

ABSTRACT:

The aggressiveness and lack of well-tolerated and widely effective treatments for advanced hepatocellular carcinoma (HCC), the predominant form of liver cancer, rationalize its rank as the second most common cause of cancer-related death. Preclinical models need to be adapted to recapitulate the human conditions to select the best therapeutic candidates for clinical

development and aid the delivery of personalized medicine. Three-dimensional (3D) cellular spheroid models show promise as an emerging *in vitro* alternative to two-dimensional (2D) monolayer cultures. 3D tumor spheroids exploit the ability of individual cells to aggregate when maintained in hanging droplets, more representative of an *in vivo* environment than standard monolayers. Furthermore, 3D spheroids can be produced by combining homotypic or heterotypic cells, more reflective of the cellular heterogeneity *in vivo*, potentially enabling the study of environmental interactions that can influence progression and treatment responses. The current research optimized the cell density to form 3D homotypic and heterotypic tumor spheroids by immobilizing cell suspension on the lids of standard 10 cm^3 Petri dishes. Longitudinal analysis was performed to generate growth curves for homotypic versus heterotypic tumor/fibroblasts spheroids. Finally, the proliferative impact of fibroblasts (COS7 cells) and liver myofibroblasts (LX2) on homotypic tumor (Hep3B) spheroids was investigated. A seeding density of 3,000 cells (in 20 µL media) successfully yielded Huh7/COS7 heterotypic spheroids, which displayed a steady increase in size up to culture day 8, followed by growth retardation. This finding was corroborated using Hep3B homotypic spheroids cultured in LX2 (human hepatic stellate cell line) conditioned medium (CM). LX2 CM triggered the proliferation of Hep3B spheroids compared to control tumor spheroids. In conclusion, this protocol has shown that 3D tumor spheroids can be used as a simple, economical, and prescreen *in vitro* tool to study tumor-stromal interactions more comprehensively.

INTRODUCTION:

The global incidence and mortality from liver cancer have continued to increase, despite advances in treatments for liver disease and most other types of cancer. In 2018, liver cancer surpassed colorectal and stomach cancer to become the 2nd most common cause of cancer-related death globally[1]. In 2020, there were more than 9,00,000 new diagnoses, accounting for 4.7% of total cancer cases worldwide[1]. This is particularly disappointing, given that the significant risk factors for the development of HCC, the most common form of liver cancer, are well characterised[2]. Cirrhosis is the most common risk factor for the development of HCC, with 80% of cases developing on the background of established cirrhosis[2]. Chronic liver diseases, which progress to cirrhosis, and consequently HCC, include Hepatitis B virus (HBV), Hepatitis C virus (HCV), alcohol-related liver disease (ARLD), non-alcoholic fatty liver diseases (NAFLD) – the latter attributed to obesity and type 2 diabetes mellitus (T2DM)[2,3]. The current management protocols for HCC are stage-dependent and limited for those with advanced cancer, who most often have a poor outcome[4]. There have been significant advances using kinase inhibitors and, more recently, immune-oncology treatments, although realistically, benefit a minority of patients with advanced liver cancers[5]. Moreover, there is concern that HCCs arising in patients with NAFLD – the most rapidly growing underlying cause, accounting for more than 50% of newly diagnosed HCC cases in western nations, may be more resistant to Programmed death 1 (PD1) checkpoint inhibitor therapy[6].

There has been a massive investment in clinical trials for patients with HCC, including significant improvements in clinical trials and their endpoints[7]. After a decade of failures, these investments have started to change the opportunities for patients. However, the reality is that the overall proportion of responders remains relatively poor, with patients included in trials often poorly

represent those cared for in the clinics. The danger is that the advances are costly and benefit the few rather than the many. As more candidate therapies emerge for single-use or combination, it is essential to have preclinical models more predictive of *in vivo* responses. These are likely to be models that incorporate additional factors contributing to the variability seen in patient responses that better reflect human HCC heterogeneity and pathological complexity[8]. Systems that recreate the *in vivo* pathophysiological conditions of HCC are needed to help understand the biology of tumor evolution, growth, and progression. The existing experimental models of chronic liver diseases and HCC usually fall under three main categories: *in vivo* animal-based models (reviewed in[9]), *in vitro* cultures[10], and *ex vivo*[11,12] models. Animal-based approaches are extensively used to study chronic liver diseases, including HCC; however, the genetic variability, high running costs, and the different immune system between species are among the main limitations for applying such models[9]. While some *ex vivo* models provide an excellent tool for focusing on human tissues compared to other *in vitro* cell line models, tissue availability and the limited experimental time course obstruct their utilization on a large scale.

On the other hand, the *in vitro* cell line models remain a good option for scientists working with limited resources, with a lesser need to have a constant supply of fresh human tissues[10]. These models also provide a tool that can be used as a first screen to help with target validation of drug selection before proceeding to more complex *in vivo* models. The recent modification of the traditional 2D monolayer cultures into 3D cultures has improved the efficacy of these *in vitro* models[13,14].

3D *in vitro* models can recapitulate critical features seen in human normal and pathological conditions. Under physiological conditions, signal transduction is initiated through cellular crosstalk and interaction with other connective tissue molecules, namely, the extracellular matrix (ECM) proteins, forming a 3D interaction network[15,16]. The tumor evolves in a 3D spherical form during malignant transformation, for which oxygen and nutrients are readily abundant in non-tumor/tumor interphase. At the same time, hypoxic conditions predominate at the tumor core. This heterogeneity in nutrient availability results in the activation of spatially distinct signaling and metabolic pathways that regulate tumorigenesis. These conditions are poorly recapitulated in the conventional 2D monolayer cultures[14], in which cells grow on stiff culture plastic in a physiologically irrelevant fashion. Cancer cells also communicate with other non-parenchymal cells, the primary source of ECM, growth, and invasion signaling within the tumor microenvironment. Unlike 2D cultures, 3D *in vitro* models can provide a more suitable platform to study this tumor-stromal interaction[17].

3D models are widely used in the HCC field, and they vary in the way the micro-tissue is formed[18–23]. Most of these models used either the ultra-low binding plates[18–22] or trans-wells[23] in the process of spheroid formation. The protocol described introduces the hanging droplet technique as an alternative, plastic-free, and cost-effective *in vitro* 3D tumor spheroid model. This may facilitate assessing the paracrine and autocrine roles of fibroblasts on the proliferation of the tumor cells in a 3D format.

PROTOCOL:

1. Cell preparation

1.1. Perform all the experiments under sterile conditions in Class II laminar flow microbiological safety cabinet (see **Table of Materials**).

1.1.1. Turn on the hood and allow for the stabilization of the airflow.

1.1.2. Thoroughly spray the interior hood surface with 70% ethanol to eliminate any possible contamination from previous users.

1.1.3. Prepare 5% of a disinfectant solution in a 500 mL glass beaker. Discard any cell supernatant or cell debris inside the solution.

1.1.4. Thoroughly clean all the micropipettes and tip boxes with 70% ethanol.

1.2. Prepare fresh cell culture media by supplementing Dulbecco's modified Eagle's medium (DMEM) high glucose media with 10% heat deactivated fetal bovine serum (FBS), 1% penicillin/streptomycin (100 unit/mL of penicillin and 100 µg/mL of streptomycin), and 2 mM L-glutamine. For the LX2 hepatic stellate cell line, reduce the concentration of the FBS supplement to 2%.

1.3. Warm culture media on beads before initiating the experiment.

1.4. Take Huh7 and Hep3B HCC tumor cell lines and COS7 and LX2 fibroblast cell lines from their storage rack in liquid nitrogen. Rapidly defrost cryopreserved cells.

1.5. Dilute thawed cells with 2 mL of fresh culture media. Centrifuge cells at 200 x *g* for 4 min at room temperature. Discard the supernatant and resuspend the cell pellet in 1 mL of fresh warm culture media.

1.6. Seed cells in T75 cell culture flask. Incubate the cells in a cell culture incubator in 5% CO_2 at 37 °C in 95% humidified conditions until cells reach 60%–70% confluency.

2. Cell collection

2.1. Aspirate culture media and wash cells three times with phosphate buffer saline (PBS).

2.2. Add 2 mL of pre-warmed 1x Trypsin to detach adherent cells from the bottom of the T75 flasks. Incubate at 37 °C in an incubator for 4 min.

2.3. Inactivate trypsin by adding 4 mL of complete culture media. Collect the cell suspension and centrifuge cells at 200 x *g* for 4 min at room temperature. Discard the supernatant and resuspend the cells in 4 mL fresh culture media.

3. Cell counting

3.1. Gently vortex the cell suspension to ensure homogenous distribution of cells in the centrifuge tube.

3.2. Using a 10 µL pipette, mix 10 µL of cell suspension with 10 µL of Trypan blue. Gently pipette the mixture up and down four times to ensure complete staining of the outer cell surface with the dye.

3.3. Count the number of cells using a hemocytometer.

3.3.1. First, place a coverslip over the hemocytometer counting area before loading the stained cell mix.

3.3.2. Place the pipette tip containing the cell mix into the V groove of the hemocytometer. Gently expel the tip content into the counting slide.

3.3.3. Leave the slurry to settle for a couple of minutes before fixing it on the microscope stage for cell counting.

NOTE: To avoid double-counting, only count the cells on the two sides of the large square.

3.3.4. Count in cells overlapping the top or the right ruling and avoid those overlapping the bottom or the left ruling.

3.4. Calculate the total number of cells.

NOTE: Cell number per mL= Cell count x $\frac{\text{Dilution factor}}{\text{Number of squares}}$ x 10^4

4. Collection of fibroblast conditioned media (CM)

4.1. Aspirate culture media and wash the LX2 cells three times with PBS.

4.2. Add 2 mL of pre-warmed 1x Trypsin to detach adherent cells from the bottom of the T75 flasks. Incubate the flask at 37 °C in an incubator for 4 min.

4.3. Inactivate trypsin by adding 4 mL of complete culture media. Collect the cell suspension and centrifuge cells at 200 x *g* for 4 min at room temperature. Count the cells as per step 3.

4.4. Seed 1 x 10^6 LX2 cells in 10 cm^3 dishes for 48 h at 37 °C.

4.5. Collect the fibroblast CM after 48 h. Centrifuge at 200 x *g* for 4 min at room temperature

to pellet any floating cells. Sterile filter the CM using a 0.22 µm filter fixed on the bottom of 20 mL syringes.

4.6. Collect the supernatant CM. Aliquot the CM into 2 mL tubes and store at -80 °C for further applications.

NOTE: The solution can be stored for 6 months at -80 °C.

5. Validating cell densities for perfect spheroids

5.1. Aspirate culture media and wash the HCC cell lines three times with PBS.

5.2. Add 2 mL of pre-warmed 1x Trypsin to detach adherent cells from the bottom of the T75 flasks. Incubate at 37 °C in an incubator for 4 min.

5.3. Inactivate trypsin by adding 4 mL of complete culture media. Collect the cell suspension and centrifuge cells at 200 x *g* for 4 min at room temperature.

5.4. Count the cells as per step 3.

5.5. Pipette different densities from the tumor cell lines (12000, 6000, 3000, 1500, 1000, 750, 500, 250, and 125 cells) in 20 µL of media on the interior surface of a 10 cm^3 lid of a Petri dish.

5.6. Add 10 mL of sterile PBS to the bottom of the dish to provide humid conditions for the process of spheroid formation.

5.7. Invert the lid of the 10 cm^3 dish to allow the media, including the cell suspension, to hang over a humid environment. Leave the hanging droplets for 3 days.

5.8. Take images of the spheroids at 50x magnification using an inverted microscope 3 days after hanging the original droplets.

6. Heterotypic tumor/stromal spheroids

6.1. Suspend 1500 Huh7 HCC cells with 1500 COS7 mammalian fibroblast cells (1:1 ratio) in hanging droplets to form spheres. Add 10 mL of sterile PBS to the bottom of the dish to provide humid conditions for the spheroids.

6.2. Invert the lid of the 10 cm^3 dish to allow the media, including the cell suspension, to hang over a humid environment. Leave the hanging droplets for 3 days.

6.3. Take images of the spheroids using an inverted microscope from day 3 until day 10 of culture.

6.3.1. Put the 10 cm^3 dish on the microscope stage. Adjust the magnification of the microscope at 50x for all spheroids.

6.3.2. Open the microscope software on the attached computer and adjust its focus to have a clear image of every spheroid. Use the **Capture Tool** on the microscope software to save the acquired pictures.

7. Homotypic Hep3B spheroids in LX2 CM

7.1. Suspend 3000 Hep3B HCC cells in the hanging droplets to form spheres. Add 10 mL of sterile PBS to the bottom of the dish to provide humid conditions for the spheroids.

7.2. Invert the lid of the 10 cm^3 dish to allow the media, including the cell suspension, to hang over a humid environment. Leave the hanging droplets for 3 days.

7.3. Transfer Hep3B spheroids into 20 µL of fresh CM from LX2 cells in hanging droplets.

NOTE: Use sterile autoclaved unfiltered 200 µL pipette tips in the process of spheroid transfer to avoid any disruption or injury to the formed spheroids. This is also to eliminate any residual cells that remain unattached to the main single spheroid.

7.3.1. Use an autoclaved 20 µL pipette for the transfer process. Adjust the pipette volume to 2 µL. Attach the pipette tip to the pipette.

7.3.2. Invert the lid of the 10 cm^3 dish on which the spheroids were formed. Fix the lid on the stage of a light microscope. Adjust the fine focus of the microscope to make each spheroid visible.

7.3.3. Carefully empty the air from the micropipette by pressing the plunger button. Insert the pipette tip in the droplet, including the spheroid, to be transferred. Get very close to the spheroid without touching it with the tip.

7.3.4. Gently release the pressure on the plunger button to allow the suction of the spheroid into the micropipette tip in 2 µL media.

7.3.5. Transfer the spheroid into a new droplet hanged on a new 10 cm^3 dish, having new media/conditioned media/treatment.

NOTE: Ensure that all the spheroids are successfully transferred to the new 10 cm^3 dish using the light microscope.

7.4. Take images of the spheroids at 50x magnification using an inverted microscope from the day of transfer (day 3) until day 7 of culture in LX2 CM.

8. Calculation of spheroid volume

8.1. Assign a unique numeric identifier for each spheroid so that images from matched spheroids can be captured daily.

8.2. Analyze images of the growing spheroids using an image analysis software package.

8.2.1. Open each spheroid image within the software package. Using the **Freehand** selection tool and outline each spheroid. From the **Analysis** dropdown button, select **Set Measurement**, and then **Area**. Press **OK**.

8.2.2. Manually draw a circle around each spheroid. Once the sphere is circled, press **Ctrl + M** to allow the program to calculate the spheroid area in Pixels. Convert the area of the spheroid into a volume.

NOTE: Volume of spheroid$_{mm3}$=0.09403 x $\left(\frac{\text{Spheroid area}_{\text{Pixel}} \text{ x } 0.28}{1000}\right)^{1.5}$

8.2.3. Calculate the change in spheroid volume relative to its volume on the first day of image capture.

NOTE: This is to normalize the spheroid volume to the starting volume and improve accuracy given the natural variation in the starting size.

REPRESENTATIVE RESULTS:

Cells cultured in a multi-layered 3D format more accurately reflect the complexity of the tumor microenvironment than conventional 2D cultures[24,25]. Previously, many studies have supplemented the spheroids culture media with different mitogens and growth factors[26] to initiate spheroid formation. In this study, however, the addition of fibroblasts, or their CM, provides essential mitogens and growth factors to accelerate spheroid growth.

Figure 1 depicts data from a pilot study in which Huh7 human HCC cells were seeded in a descending seeding density starting from 12,000 down to 125 cells in 20 µL fresh media for 3 days. A seeding density of 12,000 cells yielded spheroids with an asymmetric shape, which was not corrected even after halving the cell seeding density. However, spheroids created from 3000 cells looked more rounded (**Figure 1**, upper row). Further reduction of cell concentration neither succeeded in forming single spheres (125, 250, 500 cell-density spheres) nor had a regular spherical-like appearance (1000 and 1500 cell-density spheroids). It is worth mentioning that many small spheres were formed at a density of 500 tumor cells; however, only one small spheroid was captured at 50x magnification (**Figure 1**, upper row). The same optimized protocol was applied to the COS7 primate kidney fibroblast cell line (**Figure 1**, middle row). Suspending 125, 250, and 500 COS7 fibroblasts in 20 µL hanging droplets resulted in one rounded spheroid with multiple smaller spheroids, while higher cell densities (1000, 1500, and 3000) formed single semi-rounded spheroids. Similar to the Huh7 tumor spheroids, higher cell suspensions (6,000 and 12,000 cells/sphere) resulted in the formation of irregular cell aggregates, and hence higher cell

concentrations were discarded (**Figure 1**, middle row). Low Huh7/COS7 heterotypic cell suspensions (125, 250, and 500 cells/sphere) generated a single spheroid with multiple floating or semi-attached spheroids (**Figure 1**, bottom row). 1000- and 1500-cell heterotypic spheroids were semi-rounded, while a seeding density of 3000 cells (1500 per cell type) gave a perfect, rounded 3D spheroid. As noted earlier, higher cell densities resulted in the formation of aggregates rather than well-defined spheroids (**Figure 1**, bottom row). In conclusion, 3000 cell-density spheroids were rounded, similar to human HCC tumors, and were adapted for further experiments. Culturing the cell suspensions as hanging droplets for 3 days was sufficient to promote spheroid formation.

After optimizing the best cell concentration and time point for spheroid formation in the current context, the proliferative impact from co-culturing tumor and fibroblast cell lines was assessed longitudinally. **Figures 2** and **Figure 3** show Huh7/COS7 heterotypic spheroids (3000 total cell numbers per spheroid) monitored from day 3 until day 10. Homotypic Huh7 and COS7 spheroids (1500 cells each) served as controls. Starting from day 4, heterotypic spheroids grew in an ideal round-like shape compared to homotypic spheroids (**Figure 2**). The initial volume of the heterotypic spheroid was larger than that of each homotypic spheroid. The growth of spheroids was calculated as the change in their volume relative to initial volume at the day of spheroid formation to avoid normal variation in spheroid volume (day 3, **Figure 3**). Heterotypic spheroids initially showed a rapid growth phase starting from day 4 up to day 7 followed by a slower phase of growth at day 8 (**Figures 2**, upper row, and **Figure 3**). The spheroid volume decreased on days 9 and 10, possibly reflecting the depletion of nutrients or a hypoxic core and cell death.

In contrast, homotypic Huh7 and COS7 spheroids grew at a much slower rate (**Figure 2**, middle and bottom rows; **Figure 3**). Homotypic spheroids exhibited a relatively static growth curve until the fifth day of culture (two days after spheroid formation). Starting from day 6, the homotypic spheroids began to show a gradual increase in their growth curve, albeit at a significantly lower rate than that of the heterotypic spheroids (**Figure 3**). In conclusion, tumor/fibroblast heterotypic spheroids grow at a higher rate than homotypic spheroids suggesting that the direct contact of tumor and fibroblasts increases the size of the tumor spheroids.

Finally, to validate the above findings and to study the paracrine impact of mesenchymal cells on the proliferation of HCC spheroids in a liver-related context, 3-day-old homotypic Hep3B HCC spheroids were grown in regular fresh media or CM from LX2 hepatic stellate cells (**Figure 4** and **Figure 5**) for an additional 4 days. At first glance, 3000 Hep3B cells formed perfectly rounded spheroids after 3 days (**Figure 4**). Hep3B spheroids showed continual proliferation in fresh media from day 3 till day 7 (**Figure 4**, upper row). The growth rate was enhanced when Hep3B spheroids were maintained in LX2 CM (**Figure 4**, lower row). This media-dependent conversion in Hep3B spheroid growth exhibited statistical significance from day 4 up to the end of the experiment (**Figure 5**), suggesting a fibroblast-driven proliferation of tumor spheroids.

In conclusion, this study has successfully modified the existing 3D spheroid cultures to exploit the crosstalk between HCC tumor cells and different fibroblast cell lines and investigate the proliferative significance of this direct and indirect cellular interaction (**Figure 6**). Further

characterization of the formed spheroids is needed to improve how tumor cells interact with the surrounding microenvironment.

FIGURE LEGENDS:

Figure 1: Optimization of the optimal cell density for spheroid formation. Columns represent different cell seeding densities, and rows represent spheroids formed from Huh7 cells (top row), COS7 cells (middle row), and Huh7/COS7 heterotypic cells (bottom row). Images represent spheroids formed after suspending 125, 250, 500, 1000, 1500, 3000, 6000, and 12000 cells (from left to right) in 20 µL media for 3 days. The pilot study included two spheroids per condition, and the images were taken at 50x magnification, scale bar = 200 µm.

Figure 2: Heterotypic versus homotypic spheroid growth. Columns represent the day at which spheroid images were taken, and rows show representative images for spheroids formed from Huh7 cells (top row), COS7 cells (middle row), and Huh7/COS7 cells (bottom row). The images represent the spheroids formed after suspending 3000 cells from each condition (homotypic Huh7, COS7, or the Huh7/COS7 heterotypic spheroids) of different time points from left to right. The experiment included 10 spheroids per condition, and the images were taken at 50x magnification, scale bar = 200 µm.

Figure 3: Longitudinal analysis of heterotypic versus homotypic spheroid growth. The graph shows the growth curve of heterotypic Huh7/COS7 spheroids versus homotypic Huh7 and COS7 spheroids. Data are presented as mean ± s.e.m; n = 10 independent spheroids. ** $p < 0.01$; ****$p < 0.001$.

Figure 4: Growth of Homotypic Hep3B spheroids in myofibroblast CM. Columns represent the day at which spheroid images were captured, and rows show representative images of Hep3B spheroids cultured in fresh DMEM culture media (top row) or LX2 CM (bottom row). The experiment included seven spheroids per condition (fresh media or LX2 CM), and images were taken at 50x magnification, scale bar = 200 µm.

Figure 5: Longitudinal analysis of the homotypic Hep3B spheroid growth. The graph shows the growth curve of Hep3B spheroids in fresh DMEM culture media or LX2 CM. Data are presented as mean ± s.e.m; n = 7 independent spheroids. ****$p < 0.001$.

Figure 6: Schematic representation of the spheroid formation process. The cell suspension is pipetted on the inner lid of 10 cm^3 Petri-dish. The lid is inverted and kept for 3 days to allow for homotypic or heterotypic spheroid formation. Spheroid images are taken at 50x magnification. The figure is created using a web-based science illustration tool (see **Table of Materials**).

DISCUSSION:

The context in which the experimental cell lines grow influences their gene expression profile, pathway analysis, and functional criteria. For instance, in breast cancer cells, the coordination between different oncogenic pathways is retained only if cancer cells are grown in 3D

conformation[27]. Deregulated genes in 3D melanoma and breast cancer spheroids, but not in the monolayer cells, are more relevant to the *in vivo* human tumor[28,29]. For example, β1 integrin levels in mammary epithelial cells and tumor counterparts were lower than levels grown in a 2D format[29]. Furthermore, fibroblasts in 3D structures tend to migrate distinctly in terms of morphology and speed compared to those cultured on plastic[30]. In addition, the mechanical stiffness of the growth substrate activates specific pathways that encourage the malignant transformation of normal epithelial cells *via* deregulation of the extracellular signal-regulated kinase (ERK)/Rho in epithelial cells[31]. These factors favor the transition from conventional 2D culture to 3D spheroid models, as 3D cultures are more in keeping with human disease.

The current study used conventional laboratory tools and supplies to produce a 3D tumor spheroid model. The formed spheroids responded to the proliferation signals coming from fibroblasts, as shown by their significantly increased growth. This model belongs to the multicellular tumor spheroids category. There are three other categories of 3D tumor spheroids, including tumorospheres[32], tissue-derived tumor spheres[33,34], and organotypic multicellular spheroids[35]. In multicellular tumor spheroids, tumor cells are suspended in low-adhesion conditions to allow them to aggregate together to form spheres without touching the bottom of the culture vessel[36]. Several approaches have been employed to deliver this anchorage-independent technique, ranging from rotating systems, liquid overlay techniques, and uncoated ultra-low attachment U-shaped plates[37]. In HCC, most of the *in vitro* spheroid cultures use the ultra-low attachment 24- or 96-well plates to form rounded spheroids[18–22]. This technique is, however, not cost-effective and doesn't exclude any accidental cell-plastic contact. Other systems use trans-wells[23] or liver slices[12] to produce liver micro-tissues. Using human tissues in translational work is the gold standard but not always available or accessible by many research groups. The current approach benefited from the hanging droplets theory. Cell suspension is added so that the tumor spheroids are formed in an accessible liquid-air interface to form single rounded spheres[38]. Advantages of using this technique are the lack of any cell-plastic contact and the ease of studying the autocrine and paracrine crosstalk between tumor and fibroblast cells. This model was further validated in another study deciphering the importance of the non-parenchymal TREM2 in protecting the liver from HCC development[39]. This work showed that the volume of both Hep3B and PLC/PRF5 spheroids was higher in control LX2 CM versus TREM2-overexpressing LX2 CM in a Wnt-dependent manner[39].

In the current study, fibroblasts were mixed with tumor cells before spheroid formation to investigate the proliferative impact of this co-culture. Others have added fibroblasts, endothelial cells, and immune cells with tumor cell suspension after forming a tumor spheroid to study stromal cell migration into the tumor[40,41]. The current heterotypic spheroid model showed a similar growth pattern to the previously reported models and the original *in vivo* tumor; spheroids show exponential growth followed by a delayed growth phase, most probably due to the depletion of nutrients and enlargement of the necrotic core[42]. Instead of adding growth factors and mitogens to help spheroid formation, this study used a more physiological approach by having these growth factors from direct contact with fibroblasts or their secretome in the fibroblast CM. It is essential to mention that LX2 cells can be further activated by treating with TGFβ1 or PDGF[43]. LX2 cells have been treated with 10 ng/mL TGFβ1 for 48 h before removing the

media for different experimental settings. LX2 cells were washed three times with PBS (to exclude any direct TGFβ1 effect), and then fresh media was added for another 24 h before collecting the CM. The CM collected from TGFβ1-stimulated LX2 induced the Hep3B spheroids' growth at a higher rate than the CM from control LX2 (data not shown). This flexible system can lend itself to co-cultures of different cancer cells plus/minus fibroblasts, as well as patient-derived lines. It can also offer a medium-throughput screening assay for drugs that could be quickly adopted and inserted into a translational drug discovery pipeline to inform dosing for *in vivo* studies.

A limitation of the current study is the use of the immortalized cell lines in spheroid formation rather than freshly isolated HCC tumor cells and cancer-associated fibroblasts. Another limitation is comparing the homotypic Hep3B spheroid's growth between CM from LX2 and in fresh media rather than CM from other non-fibroblast cell lines. The latter limitation could be addressed by the genetic modification of a gene of interest in the fibroblasts followed by applying the CM from wild type versus genetically engineered fibroblast to homotypic spheroids.

ACKNOWLEDGMENTS:

MYWZ is funded by the The Secretary of State for Business, Energy and Industrial Strategy and the Newton Prize 2020 as a part of the UK's Official Development Assistance "ODA" and Newton fund. SS is supported by Cancer Research UK Advanced Clinician Scientist fellowship C53575/A29959. SS, FO, and HR receive funding as part of HUNTER, funded through a partnership between Cancer Research UK, Fondazione AIRC, and Fundacion Cientifica de la Asociacion Espanola Contra el Cancer.

DISCLOSURES:

FO is a director and shareholder of Fibrofind limited.

REFERENCES:

1. Ferlay, J. et al. Cancer statistics for the year 2020: an overview. *International Journal of Cancer* (2021).
2. Llovet, J. M. et al. Hepatocellular carcinoma. *Nature Reviews Disease Primers*. **7** (1), 6 (2021).
3. Reeves, H. L., Zaki, M. Y., Day, C. P. Hepatocellular carcinoma in obesity, Type 2 diabetes, and NAFLD. *Digestive Diseases & Sciences*. **61** (5), 1234–1245 (2016).
4. Forner, A., Reig, M., Bruix, J. Hepatocellular carcinoma. *Lancet*. **391** (10127), 1301–1314 (2018).
5. Reig, M. et al. Diagnosis and treatment of hepatocellular carcinoma. Update of the consensus document of the AEEH, AEC, SEOM, SERAM, SERVEI, and SETH. *Medicina Clinica (Barc)*. **156** (9), 463.e1–463.e30 (2021).
6. Pfister, D. et al. NASH limits anti-tumour surveillance in immunotherapy-treated HCC. *Nature*. **592** (7854), 450–456 (2021).
7. Llovet, J. M. et al. Trial design and endpoints in hepatocellular carcinoma: AASLD consensus conference. *Hepatology*. **73 Suppl 1**, 158–191 (2021).
8. Llovet, J. M., Hernandez-Gea, V. Hepatocellular carcinoma: reasons for phase III failure and novel perspectives on trial design. *Clinical Cancer Research*. **20** (8), 2072–2079 (2014).

9. Brown, Z. J., Heinrich, B., Greten, T. F. Mouse models of hepatocellular carcinoma: an overview and highlights for immunotherapy research. *Nature Reviews Gastroenterology and Hepatology*. **15** (9), 536–554 (2018).
10. Nikolic, M., Sustersic, T., Filipovic, N. In vitro models and on-chip systems: Biomaterial interaction studies with tissues generated using lung epithelial and liver metabolic cell lines. *Frontiers in Bioengineering and Biotechnology*. **6**, 120 (2018).
11. Clark, A. M., Ma, B., Taylor, D. L., Griffith, L., Wells, A. Liver metastases: Microenvironments and ex-vivo models. *Experimental Biology and Medicine*. **241** (15), 1639–1652 (2016).
12. Paish, H. L. et al. A bioreactor technology for modeling fibrosis in human and rodent precision-cut liver slices. *Hepatology*. **70** (4), 1377–1391 (2019).
13. Brassard-Jollive, N., Monnot, C., Muller, L., Germain, S. In vitro 3D systems to model tumor angiogenesis and interactions with stromal cells. *Frontiers in Cell and Developmental Biology*. **8**, 594903 (2020).
14. Pampaloni, F., Reynaud, E. G., Stelzer, E. H. The third dimension bridges the gap between cell culture and live tissue. *Nature Reviews Molecular Cell Biology*. **8** (10), 839–845 (2007).
15. Kleinman, H. K., Philp, D., Hoffman, M. P. Role of the extracellular matrix in morphogenesis. *Current Opinion in Biotechnology*. **14** (5), 526–532 (2003).
16. Bissell, M. J., Radisky, D. C., Rizki, A., Weaver, V. M., Petersen, O. W. The organizing principle: microenvironmental influences in the normal and malignant breast. *Differentiation*. **70** (9–10), 537–546 (2002).
17. Ronnov-Jessen, L., Petersen, O. W., Koteliansky, V. E., Bissell, M. J. The origin of the myofibroblasts in breast cancer. Recapitulation of tumor environment in culture unravels diversity and implicates converted fibroblasts and recruited smooth muscle cells. *Journal of Clinical Investigations*. **95** (2), 859–873 (1995).
18. Shao, H. et al. A novel stromal fibroblast-modulated 3D tumor spheroid model for studying tumor-stroma interaction and drug discovery. *Journal of Visualized Experiments: JoVE*. **156**, e60660 (2020).
19. Song, Y. et al. Activated hepatic stellate cells play pivotal roles in hepatocellular carcinoma cell chemoresistance and migration in multicellular tumor spheroids. *Scientific Reports*. **6** 36750 (2016).
20. Pingitore, P. et al. Human multilineage 3D spheroids as a model of liver steatosis and fibrosis. *International Journal of Molecular Sciences*. **20** (7) (2019).
21. Kozyra, M. et al. Human hepatic 3D spheroids as a model for steatosis and insulin resistance. *Scientific Reports*. **8** (1), 14297 (2018).
22. Khawar, I. A. et al. Three dimensional mixed-cell spheroids mimic stroma-mediated chemoresistance and invasive migration in hepatocellular carcinoma. *Neoplasia*. **20** (8), 800–812 (2018).
23. Feaver, R. E. et al. Development of an in vitro human liver system for interrogating non-alcoholic steatohepatitis. *Journal of Clinical Investigations Insight*. **1** (20), e90954 (2016).
24. Wartenberg, M. et al. Regulation of the multidrug resistance transporter P-glycoprotein in multicellular tumor spheroids by hypoxia-inducible factor (HIF-1) and reactive oxygen species. *Federation of American Societies for Experimental Biology Journal*. **17** (3), 503–505 (2003).

25. Chen, R. et al. Screening candidate metastasis-associated genes in three-dimensional HCC spheroids with different metastasis potential. *International Journal of Clinical Experimental Pathology*. **7** (5), 2527–2535 (2014).
26. Venkataraman, G. et al. Preferential self-association of basic fibroblast growth factor is stabilized by heparin during receptor dimerization and activation. *Proceedings of the National Academy of Sciences of the United States of America*. **93** (2), 845–850 (1996).
27. Bissell, M. J. et al. Tissue structure, nuclear organization, and gene expression in normal and malignant breast. *Cancer Research*. **59** (7 Suppl), 1757–1763s; discussion 1763s–1764s (1999).
28. Ghosh, S. et al. Three-dimensional culture of melanoma cells profoundly affects gene expression profile: a high density oligonucleotide array study. *Journal of Cellular Physiology*. **204** (2), 522–531 (2005).
29. Delcommenne, M., Streuli, C. H. Control of integrin expression by extracellular matrix. *Journal of Biological Chemistry*. **270** (45), 26794–26801 (1995).
30. Meshel, A. S., Wei, Q., Adelstein, R. S., Sheetz, M. P. Basic mechanism of three-dimensional collagen fibre transport by fibroblasts. *Nature Cell Biology*. **7** (2), 157–164 (2005).
31. Paszek, M. J. et al. Tensional homeostasis and the malignant phenotype. *Cancer Cell*. **8** (3), 241–254 (2005).
32. Yu, M. et al. Cancer therapy. Ex vivo culture of circulating breast tumor cells for individualized testing of drug susceptibility. *Science*. **345** (6193), 216–220 (2014).
33. Weiswald, L. B. et al. Newly characterised ex vivo colospheres as a three-dimensional colon cancer cell model of tumour aggressiveness. *British Journal of Cancer*. **101** (3), 473–482 (2009).
34. Kondo, J. et al. Retaining cell-cell contact enables preparation and culture of spheroids composed of pure primary cancer cells from colorectal cancer. *Proceedings of the National Academy of Sciences of the United States of America*. **108** (15), 6235–6240 (2011).
35. Rajcevic, U. et al. Colorectal cancer derived organotypic spheroids maintain essential tissue characteristics but adapt their metabolism in culture. *Proteome Sciences*. **12**, 39 (2014).
36. Friedrich, J., Seidel, C., Ebner, R., Kunz-Schughart, L. A. Spheroid-based drug screen: considerations and practical approach. *Nature Protocols*. **4** (3), 309–324 (2009).
37. Friedrich, J., Ebner, R., Kunz-Schughart, L. A. Experimental anti-tumor therapy in 3-D: spheroids--old hat or new challenge? *International Journal of Radiation Biology*. **83** (11–12), 849–871 (2007).
38. Kelm, J. M., Timmins, N. E., Brown, C. J., Fussenegger, M., Nielsen, L. K. Method for generation of homogeneous multicellular tumor spheroids applicable to a wide variety of cell types. *Biotechnology & Bioengineering*. **83** (2), 173–180 (2003).
39. Esparza-Baquer, A. et al. TREM-2 defends the liver against hepatocellular carcinoma through multifactorial protective mechanisms. *Gut*. **70** (7), 1345–1361 (2021).
40. Dangles-Marie, V. et al. A three-dimensional tumor cell defect in activating autologous CTLs is associated with inefficient antigen presentation correlated with heat shock protein-70 down-regulation. *Cancer Research*. **63** (13), 3682–3687 (2003).

615 41. Timmins, N. E., Dietmair, S., Nielsen, L. K. Hanging-drop multicellular spheroids as a model
616 of tumour angiogenesis. *Angiogenesis*. **7** (2), 97–103 (2004).
617 42. Mayer, B. et al. Multicellular gastric cancer spheroids recapitulate growth pattern and
618 differentiation phenotype of human gastric carcinomas. *Gastroenterology*. **121** (4), 839–
619 852 (2001).
620 43. Xu, L. et al. Human hepatic stellate cell lines, LX-1 and LX-2: new tools for analysis of
621 hepatic fibrosis. *Gut*. **54** (1), 142–151 (2005).
622

Figure 1

Click here to access/download;Figure;Figure 1.png

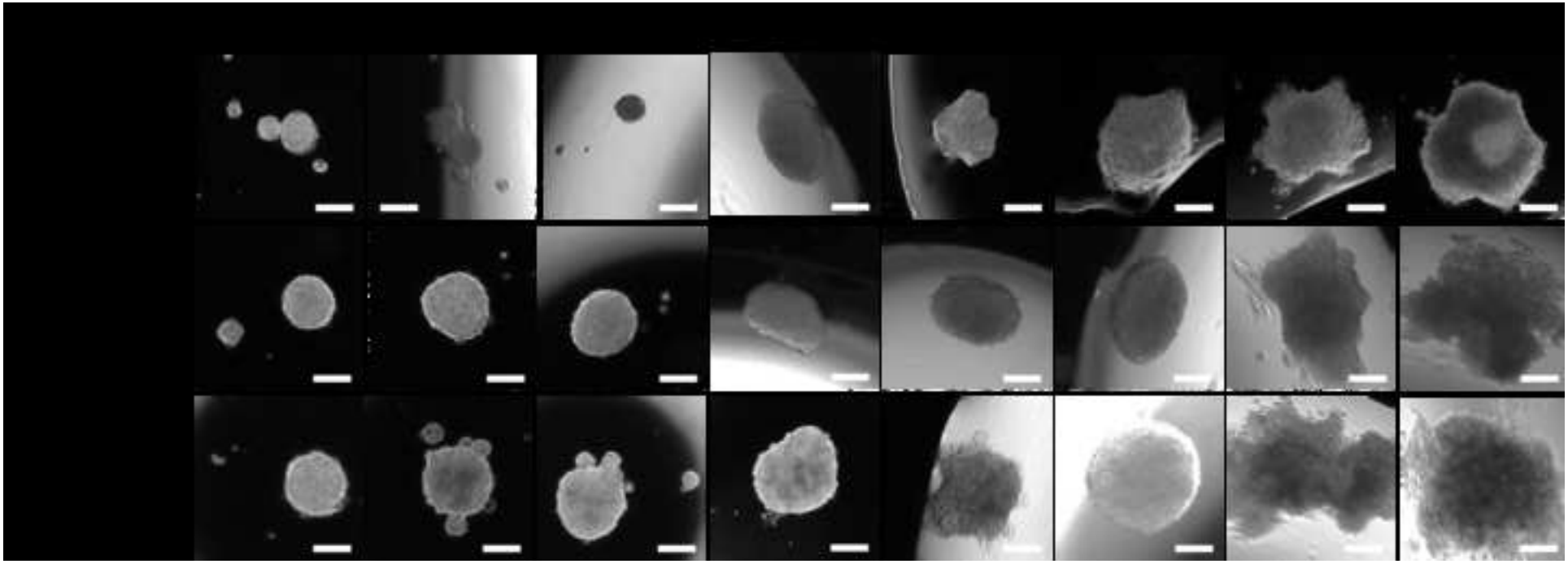

Figure 2

Click here to access/download;Figure;Figure 2.png

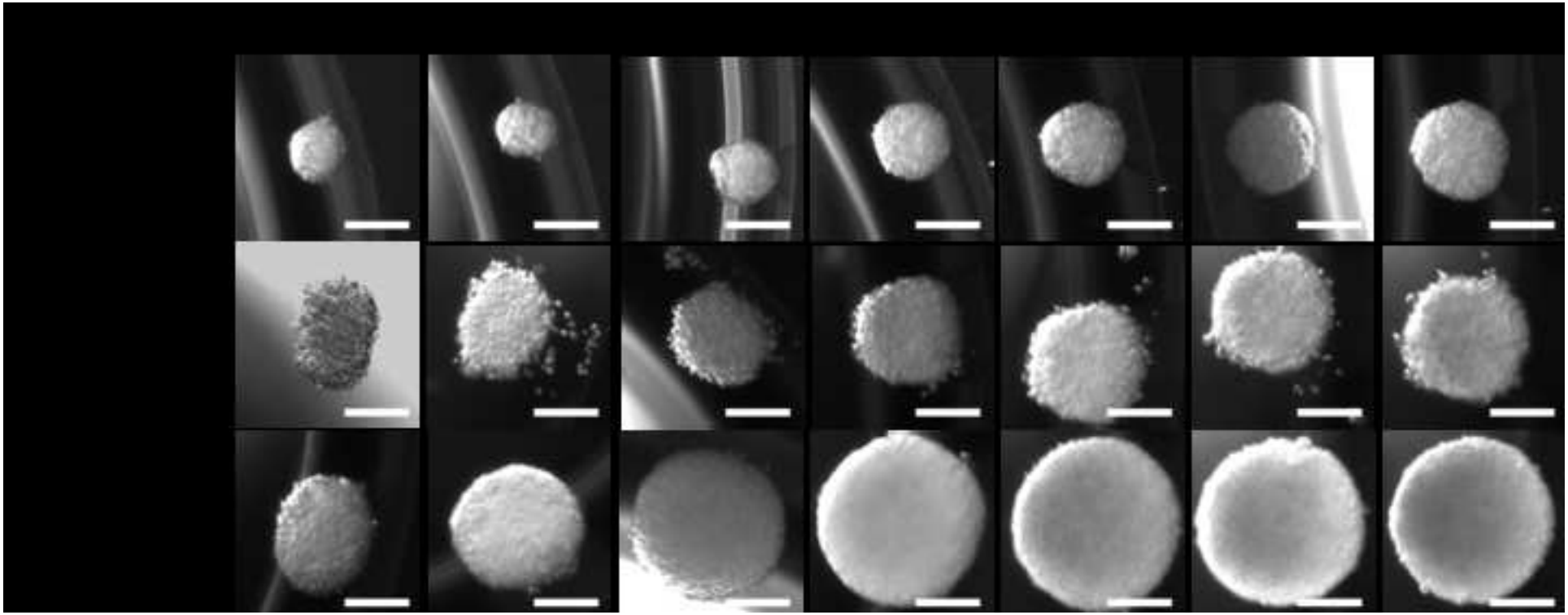

Figure 3

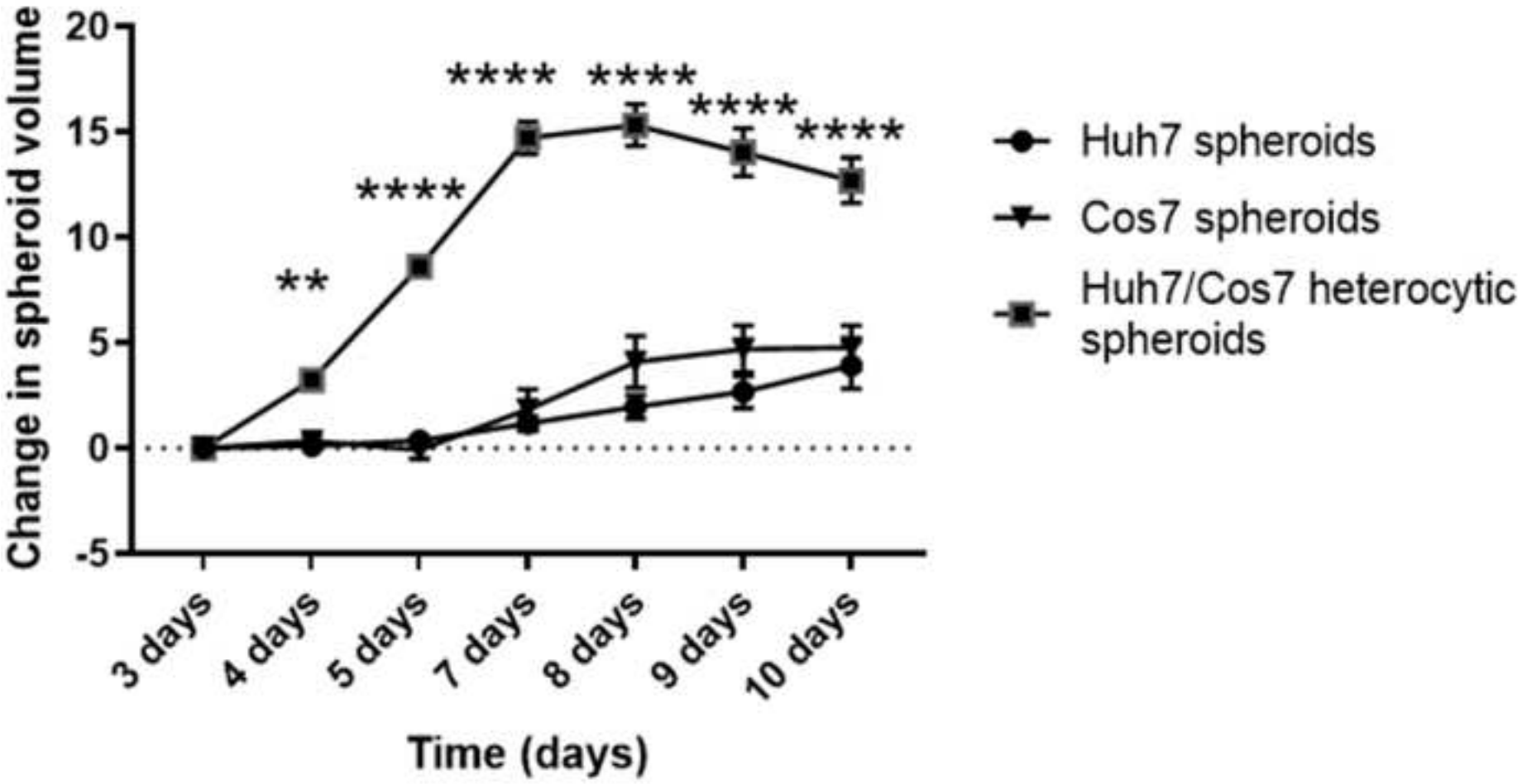

Figure 4

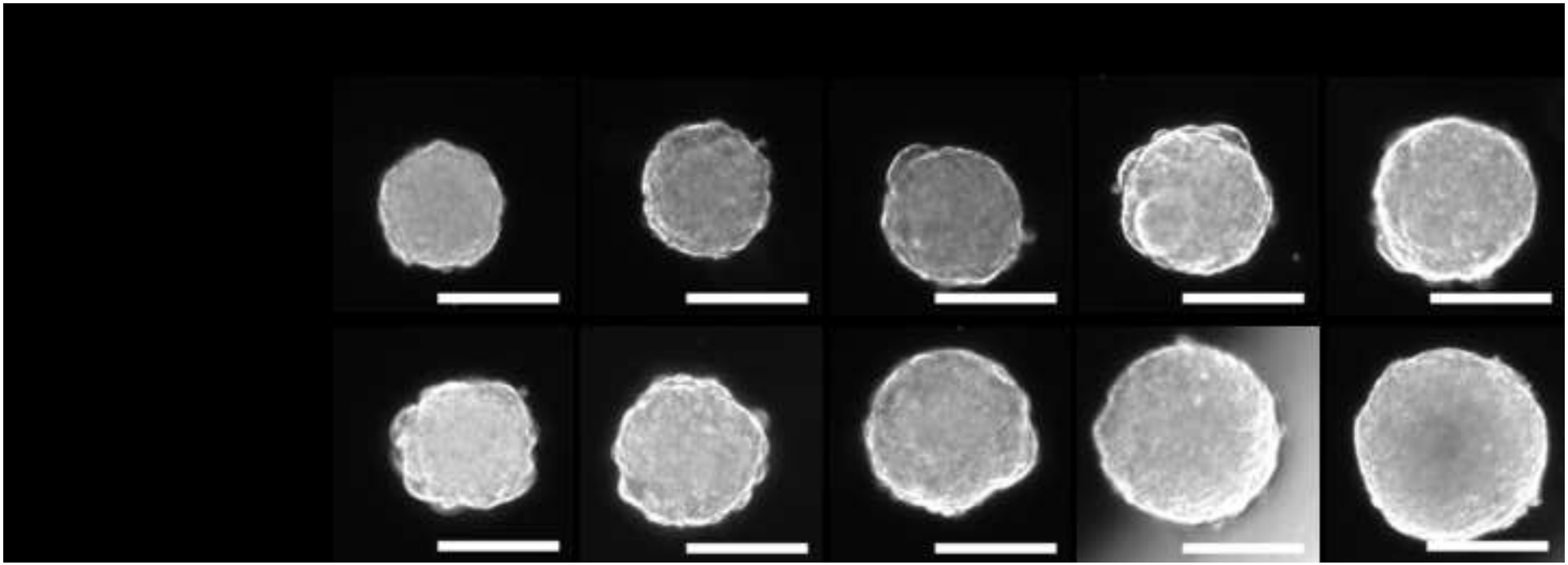

Figure 5

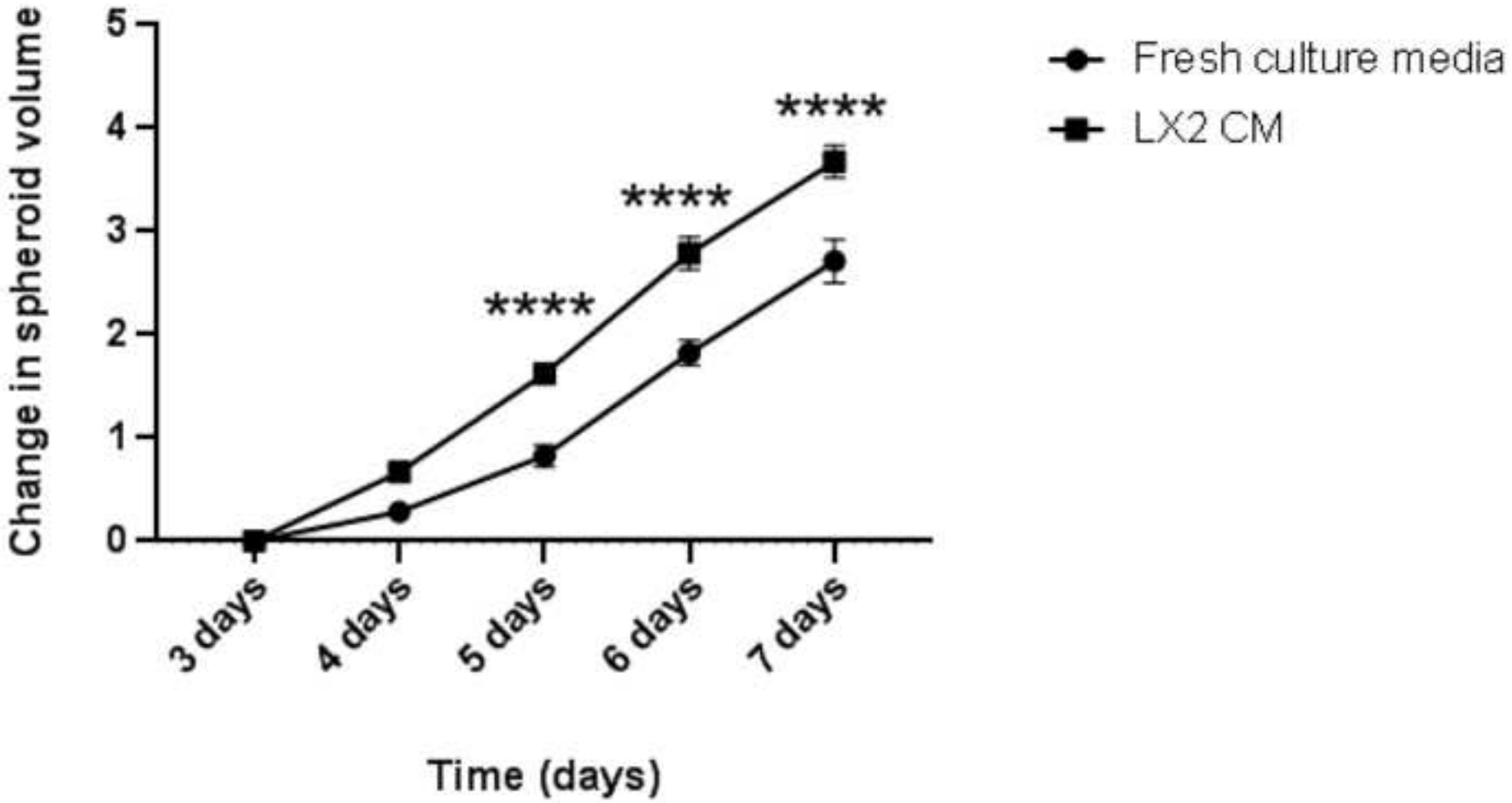

Figure 6

Click here to access/download;Figure;Figure 6.png

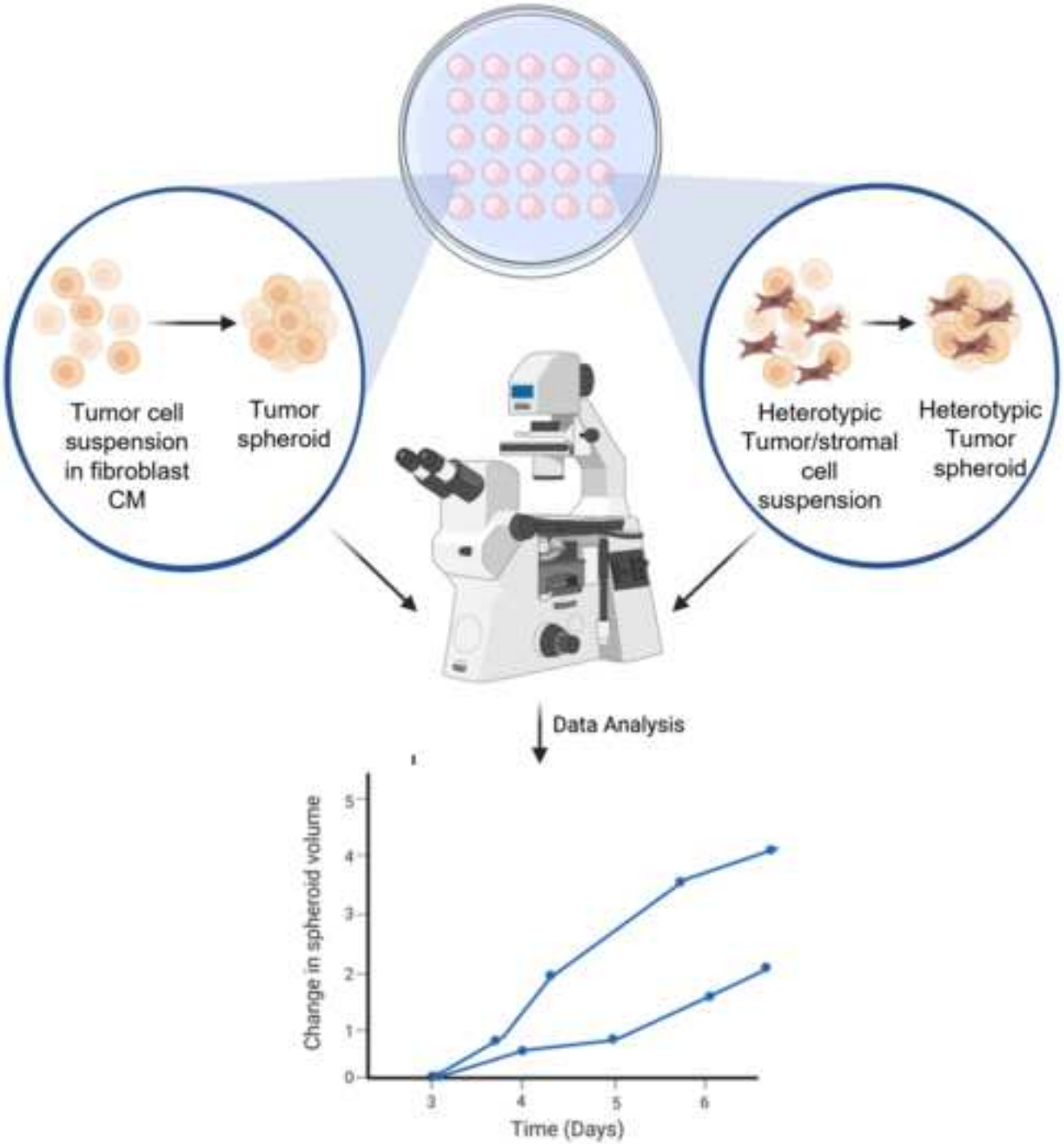

Editorial comments:

Changes to be made by the Author(s):

1. Please take this opportunity to thoroughly proofread the manuscript to ensure that there are no spelling or grammar issues. Please define all abbreviations at first use. Please use American English.

Thank you. I confirm that the manuscript was revised for spelling or grammar mistakes. Changes are tracked. The abbreviations are defined at the first use and the use of the American English is applied.

2. Please indicate corresponding author in the manuscript. Please provide an email address for each author.

Thank you. This is now added to the manuscript. Email addresses have been added to the affiliation section.

3. JoVE cannot publish manuscripts containing commercial language. This includes trademark symbols (™), registered symbols (®), and company names before an instrument or reagent. Please remove all commercial language from your manuscript and use generic terms instead. All commercial products should be sufficiently referenced in the Table of Materials and Reagents. For example: G7513-100ml; Zeiss inverted microscope; Eppendorf tubes; Excel; Graph pad prism etc.

Thank you. All the trademarks, company and software names are now deleted from the manuscript and added to the material excel file.

4. Please note that your protocol will be used to generate the script for the video and must contain everything that you would like shown in the video. Please add more details to your protocol steps. Please ensure you answer the "how" question, i.e., how is the step performed? Alternatively, add references to published material specifying how to perform the protocol action. Please add more specific details (e.g., button clicks for software actions, numerical values for settings, etc) to your protocol steps. There should be enough detail in each step to supplement the actions seen in the video so that viewers can easily replicate the protocol.

Thank you. More details have now been added to the protocol steps in main text to make the video easier to follow.

5. After including a one line space between each protocol step (section 8), highlight up to 3 pages of protocol text for inclusion in the protocol section of the video. This will clarify what needs to be filmed. This is a hard limit to ensure filming is completed in one day.

Thank you for the formatting advice. The methods section has now been adjusted to 1 line space and 3 pages are highlighted for filming the protocol.

6. Please include a scale bar for all images taken with a microscope to provide context to the magnification used. Define the scale in the appropriate Figure Legend.

The figures have now been updated and the scale bar is defined within figure legends.

7. In Figure 6, consider making the graph obtained from data analysis more realistic in terms of your protocol: what would you plot against the x and y axes?. It doesn't have to be realistic, just representative of what one expects from these experiments.

The figure has now been amended in response to this important comment.

8. Please ensure that the references appear as the following: [Lastname, F.I., LastName, F.I., LastName, F.I. Article Title. Source (ITALICS). Volume (BOLD) (Issue), FirstPage–LastPage (YEAR).] For 6 and more than 6 authors, list only the first author then et al. Please include volume and issue numbers for all references, and do not abbreviate the journal names. Make sure all references have page numbers or if early online publication, include doi.

I have downloaded the journal's style from your template word document and have applied this style on the manuscript as usual.

9. Please sort the Materials Table alphabetically by the name of the material.

The materials are now listed alphabetically.

We would like to thank the reviewers for their insightful comments and have addressed them as below. We believe that these changes have significantly improved the manuscript.

Reviewers' comments:

Reviewer #1:

Manuscript Summary:

The authors in this article recommended a simple and economical method to form tumor spheroids. Through this model, the researchers found that Cos7-cocultured Huh7 spheroids obtained an increased proliferation rate, and the CM of LX2 was able to trigger the proliferation of Hep3B spheroids. This is a good method that can definitely cut the cost of doing tumor spheroids experiments. However, I still have some questions regarding to some details in the sections of methods and results.

Major Concerns:

1. Line 181, Please provide more details how you transfered the spheroids into 20 µl of fresh CM. This step must be crucial and very tricky.

We thank the reviewer for raising this important technical point. This information has now been added to section 7.5 of the manuscript(pages 6, 7).

2. In this study, Huh7/Cos7 spheroids were made to investigated the proliferation of spheroids affected by Cos7. As LX2 and Hep3B were both originally from liver, why not consider using Hep3B/LX2 spheroids to observe the direct effect of LX2 on Hep3B?

Thank you for this important point and is relevant to disease. As a methodology paper, we wished to include an example of how to achieve optimal conditions for spheroid formation and growth; volumes and cell numbers to form both homotypic and rounded heterotypic spheroids. These parameters were from our initial optimisation work.

In a subsequent study we have successfully modulated a specific CAF target protein in the liver context of liver cancer. This is now published in GUT, and uses the same technique introduced here to create spheroids, but was modified to treat Hep3B or PLC/PRF5 spheroids with CM from control and TREM2-overexpressing LX-2 cells[1]. This highlights the transferability of the methods to other

liver cancer cell lines and provides an example of how the method can be employed to undertake mechanistic studies. This has now been referenced and included in our discussion.

Minor Concerns:

1. As we know the material of the petri dish may influence the formation and attachment of spheroids, it is necessary to point out what material is the petri dish made of in this study.

Thank you. We used Petri dish 90mm, triple vented from Greiner (catalogue number 633175), however, we haven't tested other 10cm3 dishes so we cannot exclude that they are also suitable.It is important here to consider that the idea behind the hanging droplet is to inhibit the cell contact to any plastic container to allow for more *in vivo* conditions. Once the cell suspension is pipetted onto the lid of a dish, this lid was inverted, and the spheroids were formed within the hanging droplet in a plastic-free context. Hence, we assume that there is no impact of the dish type on the behaviour or the formation of the spheroids.

2. Line 146-147, How much FBS did you add into the medium for LX2 culturing before the CM collection?

Thank you. We added 2% FBS to the LX2 culture. This information is now included in lines 144, 145 of the tracked version of the manuscript.

Reviewer #2:
Manuscript Summary:
In this study, the authors propose a 3D cellular spheroid model to investigate the tumour-stromal interactions. They generated homotypic and heterotypic spheroids maintained in hanging droplets using COS7, LX2, HuH-7, and Hep3B cells to generate growth curves for homotypic versus heterotypic tumour/fibroblasts spheroids. They showed that fibroblasts support the growth of spheroids.

Major Concerns:
1- The contribution of the technique presented in this manuscript is not clear to me as there are many previously published studies showing 3D culture models for interaction between HCC tumour cells and other cells in the tumour microenvironment such as hepatic stellate cells, immune system cells and endothelial cells (for example refs 1-6). Even one of them was published in JOVE (5). The authors should clarify this in the introduction part of the manuscript.

Thank you for this valuable comment. The last paragraph of the introduction part has now been modified to address this important point. These references are now included in the introduction and compare these studies with our developed model.

Briefly, these references indeed describe various techniques to form 3D structures using ultra *low binding 96 well plates* (REFS 2-4,6). In our manuscript, however, we introduced **hanging droplets** as a more economical method to form 3D tumour spheroids. Using the conventional 10 cm^3 dishes, the cell suspension is pipetted on the lid of a dish whose bottom was filled with sterile PBS to provide humidified conditions for spheroid growth. Inverting the lid nullifies the possibility of cell contact to the plastic dish and allows the spheroids to be formed in more physiological conditions. This model is more cost-effective compared to the use of the otherwise expensive low binding 96-well plate making it a good choice for labs where financial support is limited.

Reference 1 describes a unique model that involves different cell types present in the normal and pathologic liver conditions, however, the involvement of plastic trans-wells is one limitation of such a model. In addition, tumour usually grow in 3D spherical form making the previously mentioned model less representative to the disease conditions.

The JOVE recorded 3D model (REF 5) used 24-well plates to form melanoma spheroids, we expanded on this method by preparing homotypic and heterotypic spheroids using the hanging droplet technique.

2- Authors claimed that the collected media is a condition media after 48 hours of cultivation of LX-2. However, this media would not be conditioned because LX-2 needs to be activated to release several growth factors, pro-inflammatory factors, and many other factors that support hepatocarcinogenesis (Argemi et al, 2020, Friedman et al 2008). Otherwise, they would be quiescent cells. If authors used any procedure to activate LX-2 cells, it should be included in the material methods section.

Thank you for your comment. LX-1 and LX-2 immortal cells were derived from human hepatic stellate cells [2]. The expression of PDGFRβ on the surface of LX-2 cells and the expression of fibrosis genes including aSMA, vimentin, MMP2, TIMP1 and collagen, therefore confirming that these cells express markers consistent with activated hepatic stellate cells. Here, we followed this protocol in using CM from LX-2 cells growing on plastic at low serum conditions for 48 hours, and indeed under these conditions the CM induced spheroid growth.

The reviewer does make an excellent point, as the LX-2 cells can be further activated by disease relevant stimuli such a TGFb1 or PDGF. From our studies, spheroids grown in CM from TGFB1-stimulated LX-2 cells were larger in size than spheroids grown in control LX-2 cells (manuscript is currently submitted to another journal).We have now included new text in the discussion to highlight this point, page 11.

3- The authors propose this model as a prescreening model, however, they did not include any data representing the usefulness of the model in the manuscript. These studies should be included or this claim should be revised.

Thank you for this comment. We agree with the reviewer and this aim has now removed from the manuscript.

4- In the manuscript, the authors only present only the size of the spheroids, which is not indicative of functional formations. That's why further characterizations of spheroids are needed.

Thank you for the comment. This model was initially designed to study the impact of a particular CAF-derived protein in tumour cell growth. Our gain and loss of function studies proved the proliferative impact of this particular protein on tumour growth using spheroid volume as a readout. From this point of view, we adopted the spheroid size to represent tumour size. The use of spheroid (tumour) volume is consistent with other models like, for example, tumour volume measured in tumour xenograft models. We agree that more characterisation would be needed to further investigate the paracrine interaction between tumour and fibroblast cell lines and other functional formations. There are additional options to transfect tumour and fibroblasts with fluorescent plasmids. Spheroids can be also stored in OCT for cutting and ICC in further stages, however, we

believe that this is beyond the scope of this manuscript. This is, therefore, included as one limitation of the study (line 335 in the revised manuscript).

5- Line 246-249:Authors suggested that the direct contact between the tumour and fibroblast in heterotypic spheroids favours a proliferative niche for tumour growth, but no data in the manuscript to support this. Relevant data should be included in the manuscript.

Thank you. In figure 3, the volume of the Huh7/COS7 heterotypic spheroids was significantly higher than the volume of the individual homotypic spheroids which may reflect that the direct contact between different cell types favours tumour growth. We understand that this needs more characterisation which is difficult at the moment especially with the COVID situation. We clarified our statement by changing "favours a proliferative niche for tumour growth" to "increases the size of the tumour spheroids" in line 321 in the revised manuscript.

1. Feaver RE, Cole BK, Lawson MJ, et al. Development of an in vitro human liver system for interrogating nonalcoholic steatohepatitis. JCI Insight. 2016;1(20):e90954. Published 2016 Dec 8. doi:10.1172/jci.insight.90954
2. Khawar IA, Park JK, Jung, ES Lee, MA, Chang S, Kuh, HL. Three Dimensional Mixed-Cell Spheroids Mimic Stroma-Mediated Chemoresistance and Invasive Migration in hepatocellular carcinoma, Neoplasia, 20 (8):800-812, 2018.
3. Kozyra, M., Johansson, I., Nordling, Å. et al. Human hepatic 3D spheroids as a model for steatosis and insulin resistance. Sci Rep 8, 14297 (2018). https://doi.org/10.1038/s41598-018-32722-6
4. Pingitore P, Sasidharan K, Ekstrand M, Prill S, Lindén D, Romeo S. Human Multilineage 3D Spheroids as a Model of Liver Steatosis and Fibrosis. Int J Mol Sci. 2019;20(7):1629. Published 2019 Apr 2. doi:10.3390/ijms20071629
5. Shao, H., Moller, M., Wang, D., Ting, A., Boulina, M., Liu, Z. J. A Novel Stromal Fibroblast-Modulated 3D Tumor Spheroid Model for Studying Tumor-Stroma Interaction and Drug Discovery. J. Vis. Exp. (156), e60660, doi:10.3791/60660 (2020).
6. Song, Y., Kim, Sh., Kim, K. et al. Activated hepatic stellate cells play pivotal roles in hepatocellular carcinoma cell chemoresistance and migration in multicellular tumor spheroids. Sci Rep 6, 36750 (2016). https://doi.org/10.1038/srep36750.
7. Friedman SL. Hepatic stellate cells: protean, multifunctional, and enigmatic cells of the liver. Physiol Rev. 2008;88(1):125-172.
8. Argemi, J., Bataller, R. Hepatocyte-stellate cell synapse in alcohol-induced steatosis: another role for endocannabinoids. Nat Rev Gastroenterol Hepatol 17, 5-6 (2020). https://doi.org/10.1038/s41575-019-0233-8

Minor Concerns:
The study based on HCC, however, the studies analyzing 3D culture system using the HCC model were not included in the discussion part. Therefore the discussion should be revised.

Thank you. The discussion is now amended to add more information about the 3D spheroids in the HCC field. We have also added another reference of a manuscript that we have recently published in GUT in 2021 including the use of our developed 3D spheroid model in understanding the protective role of TREM2-expressing non-parenchymal cells on reducing the development and progression of HCC[1].

1 Esparza-Baquer, A. *et al.* TREM-2 defends the liver against hepatocellular carcinoma through multifactorial protective mechanisms. *Gut.***70** (7), 1345-1361, (2021).
2 Xu, L. *et al.* Human hepatic stellate cell lines, LX-1 and LX-2: new tools for analysis of hepatic fibrosis. *Gut.***54** (1), 142-151, (2005).

jove JOURNAL OF VISUALIZED EXPERIMENTS
1 Alewife Center #200
Cambridge, MA 02140
tel. 617.945.9051
www.jove.com

ARTICLE AND VIDEO LICENSE AGREEMENT - UK

Title of Article: A novel three dimensional spheroid model to investigate the tumour-stromal interaction in hepatocellular carcinoma

Author(s): Marco Zoh., Shishir Shetty, Alex Wilkinson, Daniel Patten, Fiona Oakley, Helen Reeves

Item 1: The Author elects to have the Materials be made available (as described at http://www.jove.com/publish) via:

☐ Standard Access ☑ Open Access

Item 2: Please select one of the following items:

☑ The Author is **NOT** a United States government employee.

☐ The Author is a United States government employee and the Materials were prepared in the course of his or her duties as a United States government employee.

ARTICLE AND VIDEO LICENSE AGREEMENT

1. **Defined Terms.** As used in this Article and Video License Agreement, the following terms shall have the following meanings: "**Agreement**" means this Article and Video License Agreement; "**Article**" means the article specified on the last page of this Agreement, including any associated materials such as texts, figures, tables, artwork, abstracts, or summaries contained therein; "**Author**" means the author who is a signatory to this Agreement; "**Collective Work**" means a work, such as a periodical issue, anthology or encyclopedia, in which the Materials in their entirety in unmodified form, along with a number of other contributions, constituting separate and independent works in themselves, are assembled into a collective whole; "**CRC License**" means the Creative Commons Attribution 3.0 Agreement (also known as CC-BY), the terms and conditions of which can be found at: http://creativecommons.org/licenses/by/3.0/us/legalcode ; "**CRC NonCommercial License**" means the Creative Commons Attribution-NonCommercial 3.0 Agreement (also known as CC-BY-NC), the terms and conditions of which can be found at: http://creativecommons.org/licenses/by-nc/3.0/legalcode; "**Derivative Work**" means a work based upon the Materials or upon the Materials and other pre-existing works, such as a translation, musical arrangement, dramatization, fictionalization, motion picture version, sound recording, art reproduction, abridgment, condensation, or any other form in which the Materials may be recast, transformed, or adapted; "**Institution**" means the institution, listed on the last page of this Agreement, by which the Author was employed at the time of the creation of the Materials; "**JoVE**" means MyJove Corporation, a Massachusetts corporation and the publisher of The Journal of Visualized Experiments; "**Materials**" means the Article and / or the Video; "**Parties**" means the Author and JoVE; "**Video**" means any video(s) made by the Author, alone or in conjunction with any other parties, or by JoVE or its affiliates or agents, individually or in collaboration with the Author or any other parties, incorporating all or any portion of the Article, and in which the Author may or may not appear.

2. **Background.** The Author, who is the author of the Article, in order to ensure the dissemination and protection of the Article, desires to have the JoVE publish the Article and create and transmit videos based on the Article. In furtherance of such goals, the Parties desire to memorialize in this Agreement the respective rights of each Party in and to the Article and the Video.

3. **Grant of Rights in Article.** In consideration of JoVE agreeing to publish the Article, the Author hereby grants to JoVE, subject to **Sections 4 and 7** below, the exclusive, royalty-free, perpetual (for the full term of copyright in the Article, including any extensions thereto) license (a) to publish, reproduce, distribute, display and store the Article in all forms, formats and media whether now known or hereafter developed (including without limitation in print, digital and electronic form) throughout the world, (b) to translate the Article into other languages, create adaptations, summaries or extracts of the Article or other Derivative Works (including, without limitation, the Video) or Collective Works based on all or any portion of the Article and exercise all of the rights set forth in (a) above in such translations, adaptations, summaries, extracts, Derivative Works or Collective Works and (c) to license others to do any or all of the above. The foregoing rights may be exercised in all media and formats, whether now known or hereafter devised, and include the right to make such modifications as are technically necessary to exercise the rights in other media and formats. If the "Open Access" box has been checked in **Item 1** above, JoVE and the Author hereby grant to the public all such rights in the Article as provided in, but subject to all limitations and requirements set forth in, the CRC License. If the "Standard Access" box

jove JOURNAL OF VISUALIZED EXPERIMENTS
1 Alewife Center #200
Cambridge, MA 02140
tel. 617.945.9051
www.jove.com

ARTICLE AND VIDEO LICENSE AGREEMENT - UK

has been checked in **Item 1** above, JoVE and the Author hereby grant to the public all such rights in the Article as provided in, but subject to all limitations and requirements set forth in, the CRC NonCommercial License.

4. **Retention of Rights in Article.** Notwithstanding the exclusive license granted to JoVE in **Section 3** above, the Author shall, with respect to the Article, retain the non-exclusive right to use all or part of the Article for the non-commercial purpose of giving lectures, presentations or teaching classes, and to post a copy of the Article on the Institution's website or the Author's personal website, in each case provided that a link to the Article on the JoVE website is provided and notice of JoVE's copyright in the Article is included. All non-copyright intellectual property rights in and to the Article, such as patent rights, shall remain with the Author.

5. **Grant of Rights in Video - Standard Access.** This **Section 5** applies if the "Standard Access" box has been checked in **Item 1** above or if no box has been checked in **Item 1** above. In consideration of JoVE agreeing to produce, display or otherwise assist with the Video, the Author hereby acknowledges and agrees that, subject to **Section 7** below, JoVE is and shall be the sole and exclusive owner of all rights of any nature, including, without limitation, all copyrights, in and to the Video. To the extent that, by law, the Author is deemed, now or at any time in the future, to have any rights of any nature in or to the Video, the Author hereby disclaims all such rights and transfers all such rights to JoVE.

6. **Grant of Rights in Video - Open Access.** This **Section 6** applies only if the "Open Access" box has been checked in **Item 1** above. In consideration of JoVE agreeing to produce, display or otherwise assist with the Video, the Author hereby grants to JoVE, subject to **Section 7** below, the exclusive, royalty-free, perpetual (for the full term of copyright in the Article, including any extensions thereto) license (a) to publish, reproduce, distribute, display and store the Video in all forms, formats and media whether now known or hereafter developed (including without limitation in print, digital and electronic form) throughout the world, (b) to translate the Video into other languages, create adaptations, summaries or extracts of the Video or other Derivative Works or Collective Works based on all or any portion of the Video and exercise all of the rights set forth in (a) above in such translations, adaptations, summaries, extracts, Derivative Works or Collective Works and (c) to license others to do any or all of the above. The foregoing rights may be exercised in all media and formats, whether now known or hereafter devised, and include the right to make such modifications as are technically necessary to exercise the rights in other media and formats.

7. **Government Employees.** If the Author is a United States government employee and the Article was prepared in the course of his or her duties as a United States government employee, as indicated in **Item 2** above, and any of the licenses or grants granted by the Author hereunder exceed the scope of the 17 U.S.C. 403, then the rights granted hereunder shall be limited to the maximum rights permitted under such statute. In such case, all provisions contained herein that are not in conflict with such statute shall remain in full force and effect, and all provisions contained herein that do so conflict shall be deemed to be amended so as to provide to JoVE the maximum rights permissible within such statute.

8. **Protection of the work.** The Author(s) authorize JoVE to take steps in the Author(s) name and on their behalf if JoVE believes some third party could be infringing or might infringe the copyright of either the Author's Article and/or Video.

9. **Likeness, Privacy, Personality.** The Author hereby grants JoVE the right to use the Author's name, voice, likeness, picture, photograph, image, biography and performance in any way, commercial or otherwise, in connection with the Materials and the sale, promotion and distribution thereof. The Author hereby waives any and all rights he or she may have, relating to his or her appearance in the Video or otherwise relating to the Materials, under all applicable privacy, likeness, personality or similar laws.

10. **Author Warranties.** The Author represents and warrants that the Article is original, that it has not been published, that the copyright interest is owned by the Author (or, if more than one author is listed at the beginning of this Agreement, by such authors collectively) and has not been assigned, licensed, or otherwise transferred to any other party. The Author represents and warrants that the author(s) listed at the top of this Agreement are the only authors of the Materials. If more than one author is listed at the top of this Agreement and if any such author has not entered into a separate Article and Video License Agreement with JoVE relating to the Materials, the Author represents and warrants that the Author has been authorized by each of the other such authors to execute this Agreement on his or her behalf and to bind him or her with respect to the terms of this Agreement as if each of them had been a party hereto as an Author. The Author warrants that the use, reproduction, distribution, public or private performance or display, and/or modification of all or any portion of the Materials does not and will not violate, infringe and/or misappropriate the patent, trademark, intellectual property or other rights of any third party. The Author represents and warrants that it has and will continue to comply with all government, institutional and other regulations, including, without limitation all institutional, laboratory, hospital, ethical, human and animal treatment, privacy, and all other rules, regulations, laws, procedures or guidelines, applicable to the Materials, and that all research involving human and animal subjects has been approved by the Author's relevant institutional review board.

11. **JoVE Discretion.** If the Author requests the assistance of JoVE in producing the Video in the Author's facility, the Author shall ensure that the presence of JoVE employees, agents or independent contractors is in accordance with the relevant regulations of the Author's institution. If more than one author is listed at the beginning of this Agreement, JoVE may, in its sole discretion, elect not take any action with respect to the Article until such time as it has received complete, executed Article and Video License Agreements from each such author. JoVE reserves the right, in its absolute and sole

discretion andwithout giving any reason therefore, to accept or decline any work submitted to JoVE. JoVE and its employees, agents and independent contractors shall have full, unfettered access to the facilities of the Author or of the Author's institution as necessary to make the Video, whether actually published or not. JoVE has sole discretion as to the method of making and publishing the Materials, including, without limitation, to all decisions regarding editing, lighting, filming, timing of publication, if any, length, quality, content and the like.

12. **Indemnification.** The Author agrees to indemnify JoVE and/or its successors and assigns from and against any and all claims, costs, and expenses, including attorney's fees, arising out of any breach of any warranty or other representations contained herein. The Author further agrees to indemnify and hold harmless JoVE from and against any and all claims, costs, and expenses, including attorney's fees, resulting from the breach by the Author of any representation or warranty contained herein or from allegations or instances of violation of intellectual property rights, damage to the Author's or the Author's institution's facilities, fraud, libel, defamation, research, equipment, experiments, property damage, personal injury, violations of institutional, laboratory, hospital, ethical, human and animal treatment, privacy or other rules, regulations, laws, procedures or guidelines, liabilities and other losses or damages related in any way to the submission of work to JoVE, making of videos by JoVE, or publication in JoVE or elsewhere by JoVE. The Author shall be responsible for, and shall hold JoVE harmless from, damages caused by lack of sterilization, lack of cleanliness or by contaminationdue to the making of a video by JoVE its employees, agents or independent contractors. All sterilization, cleanliness or decontamination procedures shall be solely the responsibility of the Author and shall be undertaken at the Author's expense. All indemnifications provided herein shall include JoVE's attorney's fees and costs related to said losses or damages. Such indemnification and holding harmless shall include such losses or damages incurred by, or in connection with, acts or omissions of JoVE, its employees, agents or independent contractors.

13. **Fees.** To cover the cost incurred for publication, JoVE must receive payment before production and publication of the Materials. Payment is due in 21 days of invoice. Should the Materials not be published due to an editorial or production decision, these funds will be returned to the Author. Withdrawal by the Author of any submitted Materials after final peer review approval will result in a US$ 1,200 fee to cover pre-production expenses incurred by JoVE. If payment is not received by the completion of filming, production and publication of the Materials will be suspended until payment is received.

14. **Transfer, Governing Law.** This Agreement may be assigned by JoVE and shall inure to the benefits of any of JoVE's successors and assignees. This Agreement shall be governed and construed by the internal laws of the Commonwealth of Massachusetts without giving effect to any conflict of law provision thereunder. This Agreement may be executed in counterparts, each of which shall be deemed an original, but all of which together shall be deemed to be one and the same agreement. A signed copy of this Agreement delivered by facsimile, e-mail or other means of electronic transmission shall be deemed to have the same legal effect as delivery of an original signed copy of this Agreement.